Analysis of Power Quality Events for Wildfire Monitoring: Lessons Learned from a California Wildfire

Hamed Mohsenian-Rad, *Fellow, IEEE*, University of California, Riverside, CA, USA
Alireza Shahsavari, *Member, IEEE*, San Diego Gas & Electric, San Diego, CA, USA
Mehrdad Majidi *Senior Member, IEEE*, San Diego Gas & Electric, San Diego, CA, USA

***Abstract*—This paper conducts an investigative analysis on the potential insights that power quality events may provide in wildfire monitoring, with a focus on grid-caused wildfires, using real-world data from a major utility in California. The analysis demonstrates two advantages of incorporating power quality events in this context. Firstly, due to their inherent sensitivity, power quality sensors capture certain important events in voltage and current waveforms that are *not* visible in fault data. Notably, a unique power quality event was discovered and characterized, potentially offering new details about the ignition that started a major fire. Secondly, it is common for multiple power quality meters at different locations to capture the same physical event, as observed at their respective locations. This can help with validating hypotheses about the underlying physical causes of the events by utilizing data from multiple datasets, such as for ignition precursor signature analysis in wildfire monitoring.**

***Keywords*: Wildfire monitoring, real-world case study, power quality data, data-driven analysis, fault data, reclosing event, spectral analysis, differential waveforms, synchro-waveforms.**

I. Introduction

Monitoring grid-caused wildfires is a critical and challenging task in the utility industry. There is a growing literature aimed at predicting, detecting, and mitigating the impact of such wildfires [1]. Here, any source of data can be valuable, including data from power systems sensors. However, so far, the focus has been mainly on the analysis of fault data, such as the data from protection relays and fault indicators. Current methods can detect faults that are likely to cause fires [2], [3], or pinpoint the location of fires that are induced by faults [4].

In this paper, we explore the idea to also use power quality data in wildfire monitoring. Power quality data is *already available* at many substations for many utilities. For instance, San Diego Gas & Electric (SDG&E) has been recording power quality data in its substations for over two decades.

Power quality meters capture not only all the faults but also a wide range of additional power quality events. Hence, they often provide a *more comprehensive* dataset compared to fault sensors. Furthermore, it is common for several power quality meters at different locations in the power system to capture the *same* event. As a result, power quality data can allow us validate our analysis by using *multiple* independent datasets.

II. Large Footprint of Wildfires on Power Quality Measurements

Power quality meters regularly record power quality events by capturing any distortions in voltage and current waveforms.

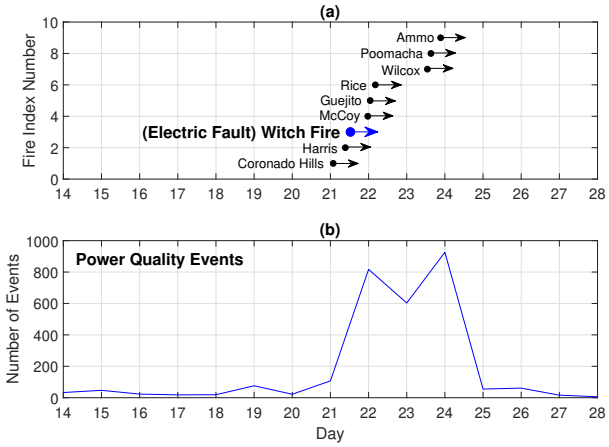

Fig. 1. The impact of wildfires on the number of power quality events across SDG&E service territory over a period of two weeks, from October 14 till October 28. Nine wildfires were reported in this period. The most destructive wildfire (Witch Fire) was caused by electric fault [5]: (a) the start date and time for each wildfire; (b) the total number of power quality events per day.

In the event of a wildfire, a significant number of waveform distortions and power quality events can be recorded.

A. Real-world Example

An example is shown in Fig. 1. This figure shows the total number of power quality events that were recorded in SDG&E's service territory between October 14, 2007 and October 28, 2007. Nine wildfires were reported in this period. The first fire started early morning on October 21. The last fire started late afternoon on October 24. The fires were mostly contained by October 25. While the number of power quality events was on average 34 events per day *before* the start of the fires, it suddenly increased to close to 1000 events per day after the fires started. Accordingly, the wildfires in this real-world example created a large footprint on power quality data. Our assessment of a number of other historical wildfires showed similar results. In all cases, the wildfire significantly increased the number of power quality events in the region.

B. Fault Data vs Power Quality Data

Of high interest in this study is Witch Fire, see the blue arrow in Fig. 1(a). This fire was caused by a fault in a Transmission Line (TL), between Creelman substation and Santa Ysabel substation [5, p. 11]. The fault that caused the fire occurred at 12:23 PM on October 21 [5, p. 13]. Two other faults had already occurred on the *same* TL on the *same* day, at 8:53 AM and 11:22 AM. Also, one fault happened three

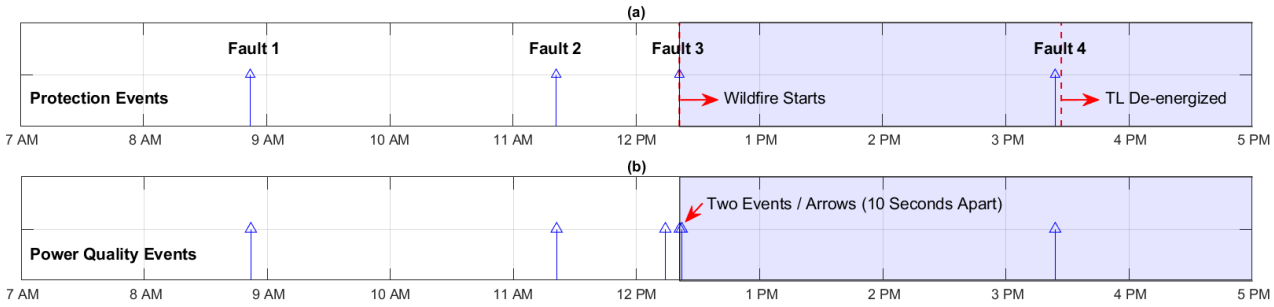

Fig. 2. Comparing the events captured by the fault recorder (protection relay) [5, pp. 12-14] versus the events captured by the power quality meter on the day when Witch Fire started. The power quality meter captured all the faults that the fault recorder captured, plus some additional events.

hours after the start of the fire, at 3:25 PM. These four faults were automatically cleared by circuit breakers. The line was automatically *reclosed* ten seconds after each fault, in all four cases. The line was *manually* de-energized after the fourth fault [5, p. 14]. The timing of the above aforementioned four faults, denoted by Faults 1, 2, 3, and 4, is shown in Fig. 2(a).

Next, consider the timing of the power quality events that were recorded on the same day at Creelman substation; see Fig. 2(b). This substation is connected to the faulted TL [5, p. 11]. All the four faults that we previously saw in Fig. 2(a) are also visible in Fig. 2(b). *In addition*, two other power quality events were recorded around the time that Fault 3 happened. One power quality event happened seven minutes before Fault 3 and one power quality event happened 10 seconds after Fault 3. By comparing Fig. 2(a) and Fig. 2(b), it is clear that the power quality data is more comprehensive than the fault data[1].

III. Problem Statement

Motivated by the findings in Section II, we seek to answer the following questions about the grid-caused Witch Fire:

- **Question 1**: Could Faults 1 and 2 have served as precursor indicators for Fault 3 that caused the fire? That is, was Fault 3 a *repetition* of the two faults that had already happened on the same day before the start of fire?
- **Question 2**: What was unique or unusual about Fault 3 (compared to the other faults) that caused the fire? As stated in [5], Witch Fire was caused by *hot particles that dispersed from the power lines* to the land in the grassy field below the power lines. What was unique in the voltage or current waveforms during Fault 3 that may indicate the occurrence of dispersing the hot particles?

Next, we will try to answer the above questions by analyzing the power quality events, in Sections IV and V, respectively.

IV. Application 1 - Precursor Signature Analysis

In this section, we seek to answer Question 1. Accordingly, we seek to examine whether Fault 1 (and Fault 2) could have potentially served as precursor indicators for Fault 3.

The raw voltage and current waveforms during these faults *cannot* be disclosed. However, we do not need to discuss the raw waveform data anyways. As it is explained in [6, Section 4.2.5], analysis of waveform events is often more insightful when it is done in *differential mode*. Suppose $v(t)$ is the raw voltage waveform during a fault or a power quality event. We define the *differential waveform* corresponding to $v(t)$ as:

$$\Delta v(t) = v(t) - v_{\text{ref}}(t). \tag{1}$$

Here, $v_{\text{ref}}(t)$ is a *reference waveform* that approximates how $v(t)$ would have looked like, had the event not occurred. In this paper, we construct $v_{\text{ref}}(t)$ by stacking up the time series of the samples in the first cycle of $v(t)$. This is shown below:

$$v(t) = \begin{bmatrix} v_1(t) \\ v_2(t) \\ \vdots \\ v_C(t) \end{bmatrix} \quad \rightarrow \quad v_{\text{ref}}(t) = \begin{bmatrix} v_1(t) \\ v_1(t) \\ \vdots \\ v_1(t) \end{bmatrix} \tag{2}$$

where C is the number of cycles in $v(t)$. By using $\Delta v(t)$ instead of $v(t)$, we remove the impact of background loads, harmonics, and other aspects in $v(t)$ that are *unrelated to the event*. This will enhance accuracy in *comparing* events.

A. Event Repetition Detection as Precursor

Fig. 3 shows the differential waveforms at the *starting cycle* of Faults 1, 2, 3, and 4. In this section, seek to systematically check whether Faults 2, 3, and 4 are the *repetition* of Fault 1. In this regard, we use two *similarity indexes*, one based on voltage and one based on current, to compare Fault 1 with *every other* power quality event that was captured between October 14 and October 28. Recall from Fig. 1 that a large number of events happened in this period. They included not only Faults 2, 3, and 4, but also several other faults, and other events, such as voltage sags, waveform distortions, etc.

The method of calculating these two similarity indexes, which are denoted by Φ_V and Φ_I, will be discussed in Section IV-B. Importantly, *lower values* for Φ_V and Φ_I indicate *more similarity* (less difference) between Fault 1 and another event.

[1]The power quality event that happened seven minutes before Fault 3 was a voltage sag. It was observed by the power quality meters at eight substations. Our analysis did *not* find this event to be relevant to the start of the fire. On the contrary, the power quality event that happened 10 seconds after Fault 3 is critical to explain the start of the fire, as we will see in Section V.

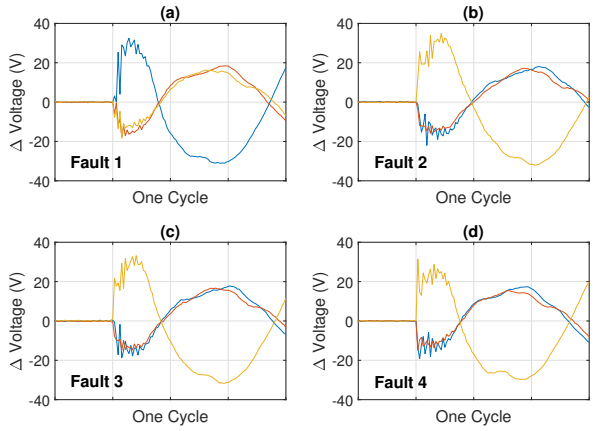

Fig. 3. Differential voltage waveforms during one cycle at the start of each fault, as seen by the power quality meter at Creelman substation.

Note 1: Since our analysis is based on power quality data, as opposed to protection data, we can conduct the similarly analysis based on power quality data from *multiple* substations. In essence, the waveforms from these various power quality meters can serve as *synchro-waveforms* to characterize the abnormality based on how its impact is captured by power quality meters at various locations in the system; see [7].

First, consider the results in Fig. 4(a). This figure is based on the differential voltage and differential current signatures of 92 power quality events that were captured between October 14 and October 28 at Creelman substation. This substation is *close* to the fault location. In Fig. 4(a), Faults 2, 3, and 4 are *distinctly separated* from *every other* event at this substation, in terms of their similarity to Fault 1. It is evident that Faults 2, 3, and 4 were *repetitions* of Fault 1. Thus, Fault 2 and 3 could have served as *precursors* to Fault 3 that caused the fire.

Next, consider the results in Fig. 4(b), which are based on the differential voltage and differential current signatures of 73 power quality events that were captured between October 14 and October 28 at Loveland substation[2]. This substation is *far* from the fault location. Nonetheless, the power quality meter at this substation captured the occurrences of Faults 1, 2, 3, and 4 as power quality events. The event signatures corresponding to Faults 2, 3, and 4 are *distinctly separated*, in terms of similarity to the event signature of Fault 1, compared to *every other* event that at this substation. This is another evidence that Faults 2, 3, and 4 were *repetitions* of Fault 1.

The conclusion from Fig. 4(b) is an *independent verification* of the similar conclusion from Fig. 4(a). This is a key outcome of using power quality data from *multiple locations*.

B. Similarity Index Calculation

In this section, we explain the method to calculate the similarity indexes that we used in Section IV-A. Due to space limitation, we only discuss Φ_V. Calculating Φ_I is similar.

[2]The number of power quality events at Loveland substation is different from the number of power quality events at Creelman substation. This is because the sensor at each substation may only see some of the events that occur in the power system, depending on the cause and location of the event.

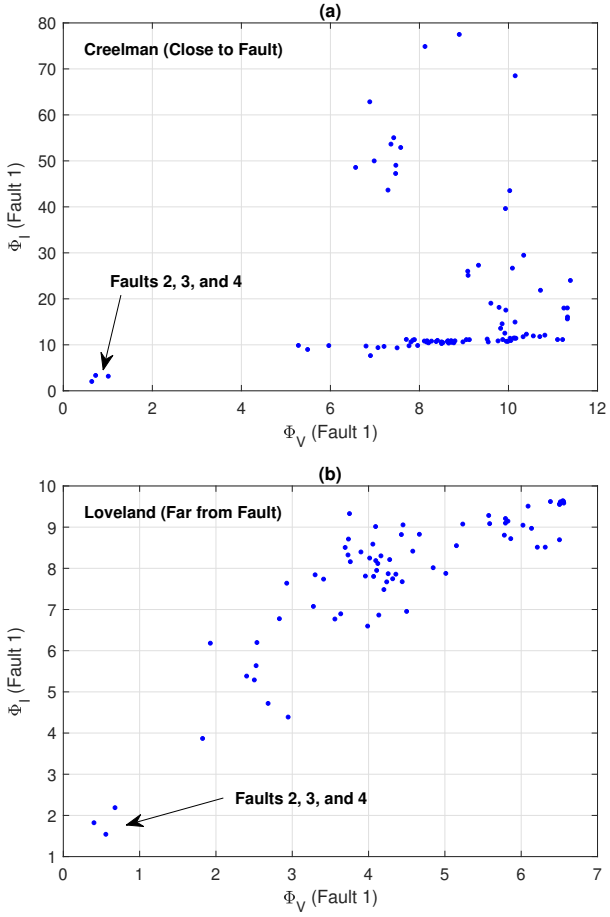

Fig. 4. The similarity indexes between the differential waveforms of Fault 1 and those of *every other* power quality event that happened from Oct 14 to Oct 28, including Faults 2, 3, and 4: (a) events at Creelman substation (close to fault); (b) events at Loveland substation (far from fault).

Let $v(t)$ be the voltage waveform that is captured by a power quality meter during an event. Let $u(t)$ be the voltage waveform that is captured by the *same* power quality meter but during *another* event. Let N be the number of samples in $v(t)$ and M be the number of samples in $u(t)$. Since $v(t)$ and $u(t)$ are captured by the *same* power quality meter, we usually have $M = N$. As stated in Section IV-A, we seek to check the similarity between $\Delta v(t)$ and $\Delta u(t)$, which are the differential waveforms corresponding to $v(t)$ and $u(t)$, respectively. Let n denote the sample number at the start of the power quality event in $\Delta v(t)$. Also, let m denote the sample number at the end of the power quality event in $\Delta v(t)$. Recall that, since we are focusing on the analysis of differential events, the start of an event is readily available; e.g., see the cases in Fig. 3, where the start of the event is at the first vertical gray line in all the four subfigures. We have $n < m \leq N$. We define:

$$\Lambda\{v(t), u(t)\} = \underset{k=1,\ldots,M-W}{\text{minimum}} \|\Delta v(n:m) - \Delta u(k:W)\|_2, \tag{3}$$

where $W = m - n + 1$. The above minimization calculates the difference between a window of length W in $\Delta v(t)$ and

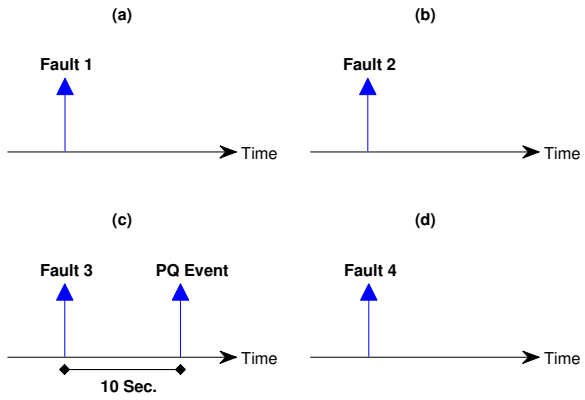

Fig. 5. Only one of the four faults was followed by a power quality event. This happened only at Fault 3, i.e., the fault that caused the fire. The sparks may have happened at *reclosing*, which happened 10 seconds after Fault 3.

a *sliding* window of length W in $\Delta u(t)$, which *slides* from the start of $\Delta u(t)$ till the end of $\Delta u(t)$. By using the sliding window, we can find the portion of the waveform of $\Delta u(t)$ that is *most similar* to the *event portion* of $\Delta v(t)$.

Suppose $\Delta v_A(t)$, $\Delta v_B(t)$, and $\Delta v_C(t)$ are the differential voltage waveforms corresponding to an event that is captured by a three-phase power quality meter. Suppose $\Delta u_A(t)$, $\Delta u_B(t)$, and $\Delta u_C(t)$ are the differential voltage waveforms of *another* event that is captured by the *same* meter. We define:

$$\begin{aligned}\Phi_V = \min\big\{\ & \Lambda_{ABC}\{v(t),u(t)\}, \Lambda_{ACB}\{v(t),u(t)\},\\ & \Lambda_{BAC}\{v(t),u(t)\}, \Lambda_{BCA}\{v(t),u(t)\},\\ & \Lambda_{CAB}\{v(t),u(t)\}, \Lambda_{CBA}\{v(t),u(t)\}\ \big\},\end{aligned} \tag{4}$$

where we check similarity based on different phase rotations across $v(t)$ and $u(t)$. Notations $\Lambda_{ABC}\{v(t),u(t)\}$, $\Lambda_{ACB}\{v(t),u(t)\}$, $\Lambda_{BAC}\{v(t),u(t)\}$, $\Lambda_{BAC}\{v(t),u(t)\}$, $\Lambda_{CAB}\{v(t),u(t)\}$, and $\Lambda_{CBA}\{v(t),u(t)\}$ are defined by rotating phases between $v(t)$ and $u(t)$. For example, we have:

$$\Lambda_{ACB}\{v(t),u(t)\} = \left\| \begin{bmatrix} \Lambda\{v_A(t),u_A(t)\} \\ \Lambda\{v_B(t),u_C(t)\} \\ \Lambda\{v_C(t),u_B(t)\} \end{bmatrix} \right\|_2. \tag{5}$$

Note that, the similarity indexes can be defined also in other forms, such as by calculating correlation or convolution.

V. Application 2 - Detection and Cause Identification with Reclosing Signature Analysis

Recall from Section V that Faults 1, 2, 3, and 4 had similar waveform signatures. This raises the following question: *what was special or unique about Fault 3 that caused the fire?*

A. Unusual Power Quality Event at Reclosing

To answer the above question, we first analyzed the *fault waveforms*. However, we did *not* find anything special in Fault 3's waveforms, compared to the other faults, to explain why Fault 3 led to fire. In fact, as far as the fault waveforms are concerned, Faults 1, 2, 3, and 4 are very similar.

Indeed, the key to answer the above question appears to be in the occurrence of a *power quality event* after Fault 3. This is shown in Fig. 5. Notice that there was a power quality event exactly 10 seconds after Fault 3. No such subsequent power quality event took place after Fault 1, Fault 2, or Fault 4.

The fact that this power quality event happened exactly 10 seconds after Fault 3 is informative by itself. In fact, per the official fire incident report, "the protection devices at each end of the line operated and opened the circuit breakers, which remained opened for *ten seconds*, and then reclosed the line, because the faults had cleared within the *ten seconds*" [5].

We will show and characterize the differential waveforms for the aforementioned power quality event in Section V-D.

Note 2: Importantly, the above power quality event is *not* visible in the fault data; because it happened 10 seconds *after* the fault. It is rather *only* visible in the power quality data.

B. Uniquely Transient Event

As the first step to investigate the unique characteristics of the power quality event at reclosing, let us define the following three metrics in order to assess the changes in the steady state characteristics of any given power quality event:

$$\Gamma_V = \big|V_{\text{after}} - V_{\text{before}}\big| \tag{6}$$

$$\Gamma_I = \big|I_{\text{after}} - I_{\text{before}}\big| \tag{7}$$

$$\Gamma_{\text{PF}} = \big|\text{PF}_{\text{after}} - \text{PF}_{\text{before}}\big|. \tag{8}$$

Here, V_{after} and V_{before} denote the magnitude of the fundamental voltage phasor after and before the event happens, respectively. We use the *first cycle* of the waveform of the captured power quality event to obtain V_{before}, and the *last cycle* of the waveform of the captured power quality event to obtain V_{after}. Similarly, I_{after} and I_{before} denote the magnitude of the fundamental current phasors after and before the event happens, respectively. Also, PF_{after} and $\text{PF}_{\text{before}}$ denote the power factors after and before the event happens, respectively.

Note 3: If *any* one of the metrics Γ_V, Γ_I, and Γ_{PF} is large, then the event has caused some major changes in the *steady state conditions*. Such events include major load switching, capacitor bank switching, faults, transformer tap changing, etc. On the contrary, if *all* metrics Γ_V, Γ_I, and Γ_{PF} are small, then the event is rather only a *transient event*; without causing major changes in the steady state conditions. Transient events are important in *diagnostics* and *prognastics* analysis in power systems, such as to detect incipient failures [6, Section 4.3].

Note 4: The power quality event that happened 10 seconds after Fault 3 was truly a transient event. This is evident from the analysis in Fig. 6. Among the 92 power quality events that were captured by the same power quality meter between October 14 and October 28, this particular event resulted in the *smallest change* in steady-state voltage, the *smallest change* in steady-state current, and the *smallest change* in power factor. That is, it manifested the smallest values for Γ_V, Γ_I, and Γ_{PF} among *all* the events. Therefore, it is very likely that this event was not related to any normal grid operation phenamena, but rather associated with some sort of *momentary* abnormality.

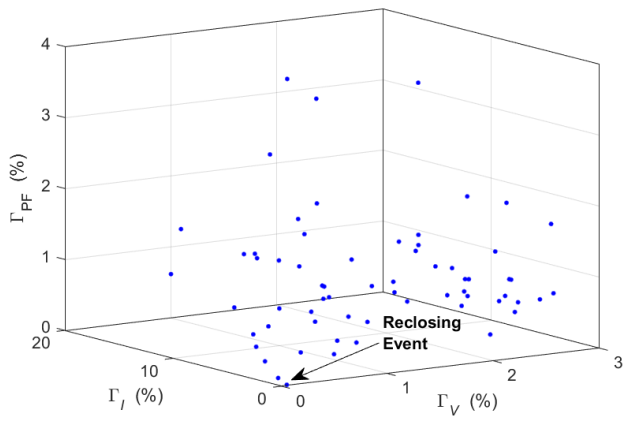

Fig. 6. The *percentage of change* in voltage, current, and power factor that happened before versus after each power quality event that was recorded at Creelman substation between October 14 and October 28. The reclosing event after Fault 3 caused the smallest change in *each* of the three quantities compared to every other power quality event during this period.

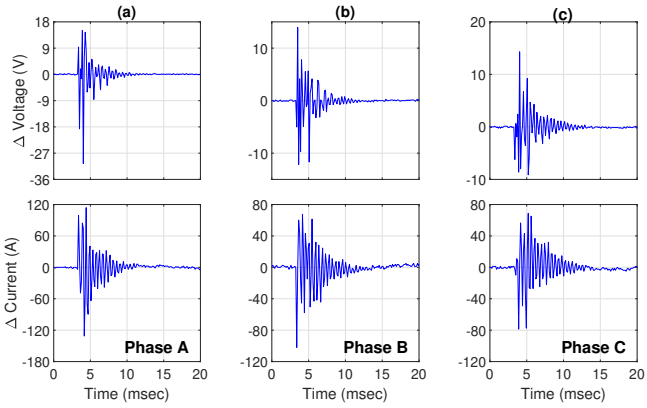

Fig. 7. The differential waveforms of voltage and current, separated for each phase, corresponding to the high-frequency damping oscillations in the power quality event that occurred at the *reclosing* after Fault 3 (also see Fig 5). The dominant frequency of the oscillations is 2.16 kHz.

C. High-Frequency Oscillations

In addition to being a truly transient event, the power quality event that happened 10 seconds after Fault 3 also manifested some unique features in its waveform. To see this, consider the differential waveforms in Fig. 7, which correspond to the three phases of the power quality event that happened at the reclosing after Fault 3. The *high-frequency oscillations* are clearly visible in these figures. By applying Fourier transform to the waveforms in Fig. 7, the dominant frequency of the oscillations are obtained at 2.16 kHz. This frequency was observed in voltage and current and across all three phases.

D. Potential Relevance to the Cause of Ignition

Recall that Witch Fire started by the *hot particles* that were dispersed from the power lines on a grassy field. Faults that cause dispersal of hot particles are often associated with *arc discharges*. Arc discharges can cause abnormalities in voltage and current waveforms, including *high-frequency oscillations* in the 2 kHz to 10 kHz range [8], [9]. These oscillations result from the rapid changes in the conductivity of the arc plasma, which causes irregular fluctuations *superimposed* on the main waveform. Therefore, it is likely that the momentary 2.16 Hz oscillations in Fig. 7 were caused by arc charging; which resulted in dispersing hot particles that started the fire.

VI. Conclusions and Future Work

Based on the analysis of power quality data from the service territory of SDG&E, it was shown that power quality events can reveal important details about wildfires that may *not* be visible in fault data. Focusing on a grid-caused wildfire, we investigated two applications of power quality data in wildfire monitoring. The first application was in *precursor signature analysis*. Our analysis was done not only at another substation that was *close* to the fault location but also at a substation that was *far* from the fault to *enhance hypothesis validation*.

The second application was in *detection and identification of ignition*. We discovered and characterized a unique power quality event at the *reclosing* after the fault that caused the fire. By developing a quantitative method, we showed that this event was truly a *transient event*, more so than *every other* power quality event that happened at the same location at anytime during the period of this study. This power quality event also demonstrated *high-frequency oscillations*. Based on the previous findings in the literature, it is likely that this power quality event was a *momentary arc charging* at the reclosing of the faulted line; which may have started the fire.

Moving forward, a key challenge is to develop algorithms that can do the same analysis in an automated fashion and in real time, using techniques in machine learning and statistics.

References

[1] S. Jazebi, F. de León, and A. Nelson, "Review of wildfire management techniques—part i: Causes, prevention, detection, suppression, and data analytics," *IEEE Trans. on*, vol. 35, no. 1, pp. 430–439, Feb. 2020.

[2] M. Zhao and M. Barati, "A real-time fault localization in power distribution grid for wildfire detection through deep convolutional neural networks," *IEEE Trans. on Industry Applications*, vol. 57, no. 4, pp. 4316–4326, Jul. 2021.

[3] J. Wischkaemper, C. Benner, B. Russell, and K. Manivannan, "Application of advanced electrical waveform monitoring and analytics for reduction of wildfire risk," in *Proc. of IEEE PES ISGT*, Feb. 2014.

[4] A. Jahromi, P. Wolfs, and S. Islam, "Travelling wave fault location in rural radial distribution networks to reduce wild fire risk," in *Proc. of the Australasian Universities Power Eng. Conference*, Australia, 2015.

[5] Public Utilities Commission of State of California, "Application of San Diego Gas Electric Company for Authorization to Recover Costs Related to the 2007 Southern California Wildfires Recorded in the Wildfire Expense Memorandum Account," Application 15-09-010, 2017.

[6] H. Mohsenian-Rad, *Smart Grid Sensors: Principles and Applications*. Cambridge University Press, UK, Apr. 2022.

[7] H. Mohsenian-Rad and W. Xu, "Synchro-waveforms: A window to the future of power systems data analytics," *IEEE Power and Energy Magazine*, vol. 21, no. 5, September 2023.

[8] J. Boksiner and E. Silverman, "Electrical cable arcing fault detection by monitoring power spectrum in distribution line," US Patent 5359293A.

[9] B. M. Aucoin and B. D. Russell, "Distribution high impedance fault detection utilizing high frequency current components," *IEEE Power Engineering Review*, vol. PER-2, no. 6, p. 1596–1606, Jun. 1982.